PROCEEDINGS OF SPIE

SPIEDigitalLibrary.org/conference-proceedings-of-spie

Land cover classification of Andean sub-basins in Colombia based on Sentinel-2 satellite images and deep learning

Darwin Arrechea-Castillo, Yady Solano-Correa, Julián Muñoz-Ordóñez, Yineth Camacho-De Angulo, Estiven Sánchez-Barrera, et al.

Darwin A. Arrechea-Castillo, Yady T. Solano-Correa, Julián F. Muñoz-Ordóñez, Yineth V. Camacho-De Angulo, Estiven Sánchez-Barrera, Apolinar Figueroa-Casas, Edgar L. Pencue-Fierro, "Land cover classification of Andean sub-basins in Colombia based on Sentinel-2 satellite images and deep learning," Proc. SPIE 12525, Geospatial Informatics XIII , 1252505 (15 June 2023); doi: 10.1117/12.2664340

SPIE.

Event: SPIE Defense + Commercial Sensing, 2023, Orlando, Florida, United States

Land cover classification of Andean sub-basins in Colombia based on Sentinel-2 satellite images and deep learning

Darwin A. Arrechea-Castillo[a], Yady T. Solano-Correa*[a,b], Julián F. Muñoz-Ordóñez[c], Yineth V. Camacho-De Angulo[a], Estiven Sánchez-Barrera[b], Apolinar Figueroa-Casas[a], Edgar L. Pencue-Fierro[a]

[a]Universidad del Cauca, Popayán, Colombia; [b]Universidad Tecnológica de Bolívar, Cartagena, Colombia; [c]Coorporación Universitaria Comfacauca, Popayán, Colombia

ABSTRACT

The Las Piedras River sub-basin, located in the department of Cauca, Colombia, is very important for the region, especially for the capital (Popayán). This is because this sub-basin contributes around 68.17% of the water supply for the city. To guarantee continuity of this resource, good management of the Water Ecosystem Services (WES) must be carried out. To this aim, periodic environmental assessments of the water resource in the region are necessary. Such Environmental Assessment WES (EAWES) is possible when an accurate and up-to-date land cover map is available. However, obtaining such a product is quite complex due to the heterogeneous conditions both in the land cover and orography of the studied region. Another impacting factor is the weather conditions of the region, that make it difficult to access the areas and/or to acquire information for land cover mapping. This research proposes a robust model, based on deep learning and Sentinel-2 satellite images, able to perform a land cover classification with reliable accuracy (>90%) at a low computational cost. A variant of a LeNet Convolutional Neural Network has been used together with features extracted from original spectral bands, radiometric indices and a digital elevation map. Preliminary results show an Overall Accuracy of 95.49% in the training data and 96.51% in the validation one.

Keywords: Deep learning, Convolutional Neural Networks (CNNs), Remote Sensing, Land Use and Land Cover, Sentinel-2

1. INTRODUCTION

Accurate and up-to-date information about Land Use and Land Cover (LULC) classification is essential for a wide range of applications, from Earth systems and climate modeling[1] to territorial and urban planning[2]. Both LULC are important for understanding the impacts of human activities on the environment and for making informed decisions about how to manage and protect natural resources. To obtain a LULC classification product using Remote Sensing (RS), it is necessary to assign a class label to every pixel or object of an image[3]. RS techniques involve the use of satellite or airborne sensors to capture information about the electromagnetic radiation emitted or reflected from the Earth's surface[4]. LULC products are continuously developing as RS and methods grow. However, there still exist low consistency among LULC products due to heterogeneity conditions, both in the LULC and in the orography of the studied regions[2].

There are various methods to generate LULC maps, each with its advantages and disadvantages. Manual techniques can be simple and straightforward approaches, but they become impractical when dealing with large study areas and high number of classes[5]. In such cases, using artificial intelligence algorithms is a more efficient alternative. Among these algorithms, traditional Machine Learning (ML) and Deep Learning (DL) are techniques that have gained popularity due to their accuracy, robustness, and ability to analyze large datasets with complex features. By utilizing these methods, one can obtain a high-quality LULC map with relatively less time and effort[6]. LULC classifications using ML algorithms have been a popular research topic in recent years, with many articles exploring this area[7–9]. Traditional ML algorithms usually work very well when the study area is small and the classes to be mapped are relatively few. Pencue-Fierro et al.[9] presented a hybrid approach for the LULC classification of multitemporal, multiregion, and multisensor Landsat data using classification and regression trees (CART) decision tree and a SVM-based clustering in cascade in order to get a total of 11 classes (including clouds and shadows). Swetanisha et al.[10] presented a study on the use of ML models to classify LULC in 7 classes. The study provides useful insights into the application of multiple ML models, including RF, SVM and KNN for LULC classification and presents a comprehensive evaluation of different models. All the above works proposed methods that rely on traditional ML supervised or unsupervised techniques, which may not be sufficient to

*tsolano@unicauca.edu.co

Geospatial Informatics XIII, edited by Kannappan Palaniappan, Gunasekaran Seetharaman, Joshua D. Harguess, Proc. of SPIE Vol. 12525, 1252505 · © 2023 SPIE
0277-786X · doi: 10.1117/12.2664340

capture complex relationships within the data. Also, the spatial resolution of Landsat imagery is not enough if you want to perform a detailed LULC classification. Therefore, a better option in terms of spatial resolution is to use Sentinel 2 (S2) images. In the research done by Park et al.[11], they applied ML algorithms like RF, XGBoost, and a LightGBM to LULC classification, and presented the model tuning process for each algorithm using S2, Landsat and a normalized digital elevation model. Razafinimaro et al. [12] used supervised classification with 6 traditional ML models. Analysis factors were used to further investigate their importance for S2, Landsat 8 and other RS information. The results showed that the KNN achieved the higher accuracy during the analysis of medium and low spatial resolution images with spectral bands lower or equal to 4. The RF completely dominated the other analysis cases. The previous works used S2 images, which allowed them to obtain detailed LULC products. Nevertheless, those studies only focused on a limited number of LULC categories, and it is unclear how well the algorithms would perform in classifying more complex or diverse LULC types. In this cases, DL techniques, such as convolutional neural networks (CNNs), have shown promising results in this field[3]. Sánchez et al.[13] compared different traditional ML and CNN algorithms to identify 19 LU classes using sequences of S2 images around a relatively small area. In this research they showed that the best results were achieved by a deep neural network containing two-dimensional convolutional layers (Conv2D) and principal component analysis (PCA). A common limitation of the above work, as others in the literature[6,14,15], is the high computational resources needed, especially when dealing with large and complex datasets, this due to complex CNNs architectures[6,14,15]. High computational resources are not always available for all research centers, making the task of LULC classification harder, if not impossible.

To deal with the different issues highlighted above, in this research we propose a simple but robust CNN architecture, capable of mapping 11 LULC in Andean and mountainous areas. We use a simple architecture that overcomes several challenges associated with more complex CNN architectures, such as high hardware costs[15] and longer wait times for results. By using this approach, we aim to provide an efficient and accessible solution for LULC classification using DL techniques[16].

2. METHODOLOGY

The proposed approach is presented in Figure 1 and consists of several stages that help to achieve an accurate and reliable result while guaranteeing a low computational time/cost. In summary, the method: (i) downloads S2 satellite images, here we talk about multiple images due to the high cloud coverage over the area that does not allow to cover it with a single S2 image; (ii) pre-processes data to guarantee homogeneity across different S2 images; (iii) creates a feature set by combining the pre-processed bands, radiometric indices, and a Digital Elevation Map (DEM), providing a more comprehensive representation of the LULCs; (iv) creates a training samples dataset that is used to both train and validate the proposed model; and (v) generates a LULC map for the studied sub-basin. Details about each of the steps is provided in the next.

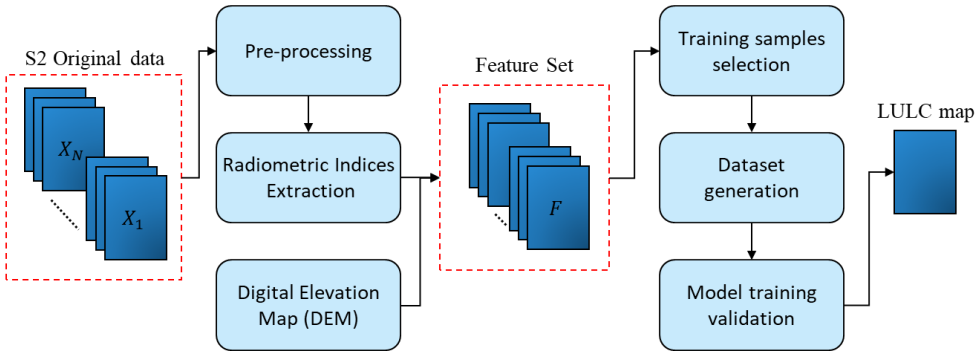

Figure 1. General block scheme of the proposed approach for LULC classification of Andean sub-basins in Colombia.

2.1 Data pre-processing

After downloading and clipping the S2 images to the area of interest, an outlier removal is conducted to eliminate pixels with values that are significantly different from the rest of the pixels in the image. This means removing pixels that have values out of expected ranges due to factors such as sensor errors, atmospheric disturbances, and other components. Next, a filtering of clouds and shadows is performed by making use of the ESA's Sen2Cor algorithm that helps to filter clouds and shadows automatically[17]. After completing the previous steps, images from different dates/tiles are radiometrically homogenized by means of histogram matching. The use of this step will allow us to use the proposed method in a more generic way for other sub-basins in the Andean region. Images are rescaled in the range [0,1], instead of keeping them in the [0,10000] one, for DL models to work in the required configurations.

2.2 LULC classes and Feature Set construction

A total of 11 LULC classes were considered for the studied area: Shrubs, Mineral extraction areas, Mixed Forest, Dense Forest, Agricultural Areas, Natural Grassland, Pasture, Planted Forest, Urban Areas, Páramo and Water. To differentiate these LULCs, supplementary features were required, in addition to the original 10 bands from S2, the B1, B9, and B10 bands were excluded from consideration, as they are specifically intended for atmospheric correction purposes. Such features were radiometric indices and DEM. Indices specific for identifying areas with vegetation, water, urban areas, and bare soil were considered to enhance DL models accuracy and efficiency[18]. A total of 16 indices were considered. For instance, the Adjusted Transformed Soil Adjusted VI (ATSAVI) and Soil Adjusted Vegetation Index (SAVI) are useful in distinguishing between natural grassland and agricultural areas[19,20], while the Green Leaf Index (GLI) and Enhanced Vegetation Index (EVI) can detect differences in forest density[21]. The Chlorophyll Index Red Edge (CIRedEdge) and Coloration Index (CI) are particularly useful in identifying different vegetation types such as páramo, shrubs, and forest[22,23]. The Normalized Difference Water Index (NDWI), the Simple Ratio - Ferrous Minerals (FM), and the Simple Ratio - Iron Oxide (IO) are effective in detecting water bodies, urban areas and mineral extraction areas[24,25]. Additionally, the DEM is also used to provide additional information.

2.3 Training samples selection

Training samples that will help to train the proposed model are selected by photointerpretation. To help with a better selection of them, the feature set composed of the 10 S2 preprocessed bands, 16 radiometric indices, and the DEM was used. The selected samples are used to automatically clip small 3x3 images for each of the 11 classes of interest in this research. These training samples present an imbalance, as shown in Table 1, due to the naturally unequal distribution of coverages in the Andean sub-basin. Therefore, an artificial balancing of the original samples is necessary to bias in the learning process. Hence, the initial samples were augmented to 26000 samples per LULC. The size of the final dataset is determined by several factors, such as the number of bands present in the original images and the number of classes used for classification. It is crucial to carefully consider these factors when building a dataset, as a larger dataset may result in more accurate classification results, but it may also require more computing power and storage space[2].

Table 1. Original distribution of the 11 LULC training samples.

LULC	Number of samples
Shrub	2148
Mineral Extraction	286
Mixed Forest	22371
Dense Forest	25809
Agricultural Areas	10958
Natural Grassland	19811
Pasture	17258
Planted Forest	15536
Urban Areas	15748
Páramo	13901
Water	3399

2.4 Proposed model setup and classification

According to the state of the art[6,14,15], increasingly complex CNN architectures are being developed to achieve highly accurate results. Such CNNs require of high computational resources to train, resulting in an increase in the economic cost of acquiring the necessary hardware to manage these models[6,26]. Therefore, in this research, we propose a robust yet simple architecture that solves these issues. The proposed model is based on the LeNet architecture[27], which is a very simple CNN with few convolutional layers, causing the computational cost associated with training this CNN to be very low. Through several experimental tests, a balance was reached between the complexity of the architecture and the robustness of the model, achieving results that outperformed larger and more complex architectures in similar tasks[6,14,15,26,28].

The construction of the CNN is done using Tensorflow API, Keras. In addition to its ease of use, Keras also provides a range of tools for monitoring and visualizing model performance[29]. This includes built-in metrics for evaluating model accuracy and loss, as well as support for callbacks that allow researchers to monitor training progress and adjust model parameters in real-time. The proposed architecture for this research comprises a total of 7 layers, which include 4

convolutional layers and 3 fully connected layers. To optimize the performance of the model, several hyperparameters were carefully selected. The batch size was set to 16, whereas the number of epochs was set to 150. Additionally, the learning rate was set to 0.0005. It is important to note that the selection of hyperparameters can significantly impact the performance of the model, and as such, they should be carefully tuned to achieve optimal results. Other parameters such the activation function was set with a ReLU for all convolutional layers. A kernel size of 3x3 was considered, padding was set to "Same", pooling was set to "Max Pooling" and learning rate to 0.25 for all convolutional layers.

3. STUDY AREA AND DATA

The study area selected for this research is the Las Piedras River sub-basin, located in the southwest part of Colombia (see Figure 2). The Las Piedras River sub-basin[30] covers an area of approximately 66 km^2 and is part of the larger Cauca River basin[18]. This sub-basin is characterized by a rugged topography, with steep slopes and narrow valleys. The main river, Las Piedras River, originates in the high Andean mountains and flows towards the southwest before merging with the Cauca River. The sub-basin is home to a rich array of flora and fauna, including several endemic species, and provides important ecosystem services such as water supply for agricultural and domestic use[30].

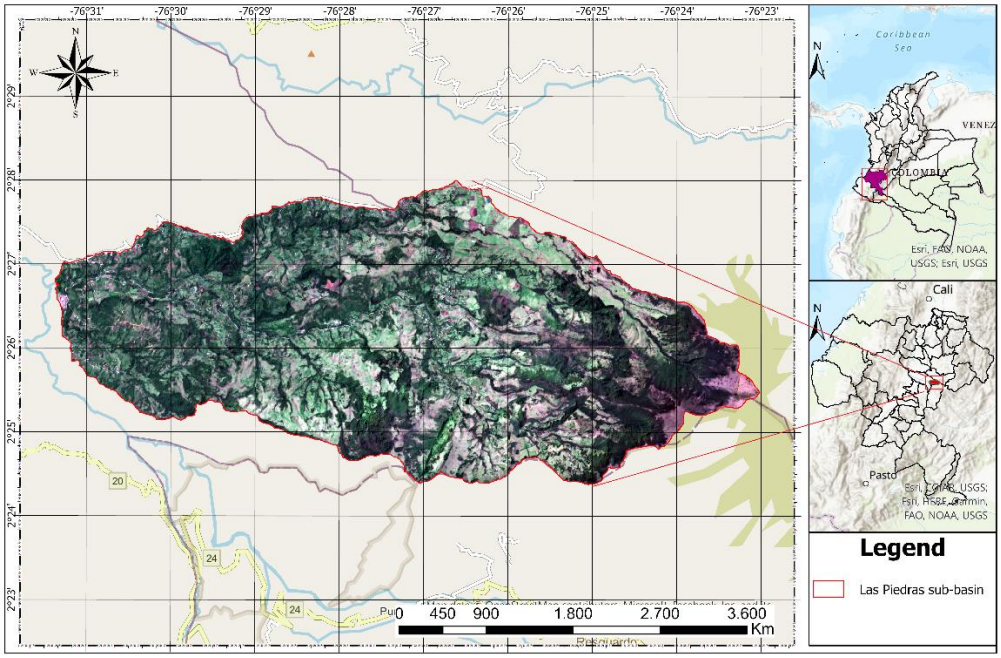

Figure 2. Study area location.

The proposed approach is developed for its application over images acquired by the S2 series satellite (up to 10m spatial resolution)[31]. The study area is located within the intertropical convergence zone, which is an area near the equator where trade winds from the northern and southern hemispheres converge. This convergence often results in the formation of cumulus clouds, which can lead to high levels of cloud cover in the region[32]. Therefore, obtaining clear images of the area of interest is challenging due to the frequent presence of clouds. The most recent images of the study area, without significant cloud coverage were obtained in 2020 and were used in the study. To generate images that cover the entire area without any cloud or shadow interference, it was essential to merge two images: S2A in orbit R068 from February 2nd of 2020 and S2B in orbit R025 from August 1st of 2020. Both images correspond to the T18NUH tile. The images were downloaded from the European Space Agency (ESA) website at Level-2A[33]. Additionally, a DEM with a resolution of 12.5 meters (acquired by ALOS PALSAR) was downloaded from the Japan Aerospace Exploration Agency (JAXA)[34]. The DEM was acquired between 2010 and 2011 and resampled to 10 meters for compatibility with the S2 data.

4. RESULTS

A total of four metrics were employed to evaluate the accuracy of the proposed approach: Overall Accuracy (OA), precision, recall, and kappa coefficient. The proposed model was trained 30 times using a large dataset and obtaining an

OA of 96.06% in the validation data for all the tests. Following the central limit theorem[35], the model training process was validated. In the best case, our model achieved an OA of 95.49% on the training data and an OA of 96.51% on the validation data. Notably, our model was particularly successful in accurately classifying the LULC categories for the study area, especially for LULC classes with more artificial samples, such as mineral extraction and agricultural areas. It was expected that the model would perform well on LULC categories such as "dense forest" and "mixed forest" because they had the most original samples available. However, it turned out that these two categories had the poorest recall scores, which indicates that the model encountered challenges in distinguishing between the subtle differences in spectral signatures that exist within these classes. Despite the availability of a relatively large number of original samples, these challenges may have contributed to the lower recall scores observed for the "dense forest" and "mixed forest" LULC classes. Regardless facing these challenges, the DL model performed remarkably well, as evidenced by a kappa coefficient of 0.962, and overall precision of 96.58% and an overall recall of 96.52%.

4.1 Influence of kernel size and LULC map

To establish the perfect balance between model complexity and dataset characteristics, various parameters combinations were tested. The kernel size used to construct the dataset was one of the most influential variables, especially in the qualitative result of the LULC classification. It determined whether the images would be small, such as 3x3, or large, such as 11x11. When using a relatively large kernel size, such as 11x11 (or larger), the quantitative accuracy was slightly higher than when using a small kernel size. However, the time required to process this information increased significantly, and the qualitative results accuracy decreased, resulting in an inadequate classification as shown in Figure 3(b). In general, the classification failed to reflect the thinner details that can be observed by photointerpretation in the S2 images in that sub-basin Figure 3(a). LULC such as narrow rivers and narrow roads are not identified by the algorithm under this configuration, as these land covers are underrepresented when a dataset with a large kernel size is constructed. Other classes such as shrubs, pastures and natural grassland are also inaccurately represented by the algorithm. To improve the classification result, other tests were conducted by increasing the kernel size to form the dataset images. However, there was no improvement, so the kernel size was reduced to 3x3, resulting in a significant qualitative improvement, shown in Figure 3(c). Under this configuration, the model performance was outstanding, even mapping small rivers and small roads accurately (OA of 96.51%). Which is a significant advancement in this type of work since in other similar LULC classification research, this has not been possible[9,36].

4.2 Performance Evaluation: CPU vs GPU

To evaluate the performance of the proposed approach for LULC classification using a simple but robust DL model, a comparison of applying the model with a CPU vs a GPU was carried out. The proposed model was trained in both a cutting-edge GPU (NVIDIA RTX 3090) and a standard CPU (Intel(R) Core (TM) i9-9900K CPU @ 3.60GHz). The required time was of ~13h with CPU vs ~5h with GPU. The results show that, for the dataset built for this research and with the simple architecture implemented, it is not necessary to have the latest computational resources to train the architecture. While using a powerful GPU can significantly reduce the training time, the difference in results was not significant enough to justify the cost of a top-of-the-line GPU for this project.

5. CONCLUSIONS

A simple, yet robust, DL based LULC classification method that works with S2 images acquired over Andean sub-basins has been presented. The results showed that, while DL models do require large amounts of data to be trained in an appropriate way, there is no need for complex CNNs architectures to obtain outperforming results. This finding has implications for both researchers and practitioners who may be limited by budget, thus showing that accurate results are achievable with moderate computational resources. The success of the proposed approach depends largely on the quality of the data used, the pre-processing performed, and the careful selection and tuning of the CNN hyperparameters. As future developments, it would be interesting to evaluate the operability of the proposed approach over larger Andean sub-basins that may bring new challenges (i.e., less cloud free images to work with).

ACKNOWLEDGMENTS

This research received support from various projects including the "Young Researchers and Innovators in the Cauca Department", "Development of Food and Water Security Strategies for the Economic Reactivation of Rural Communities," "Bioeconomic Strengthening for Social and Productive Reactivation," and the "Water Security and Sustainable

Development Hub." These projects were funded by the science ministry in Colombia and the UK Research and Innovation's Global Challenges Research Fund (GCRF) [grant number: ES/S008179/1]. The authors also express their gratitude to the Universidad del Cauca and Universidad Tecnológica de Bolívar for their support during the development of this research.

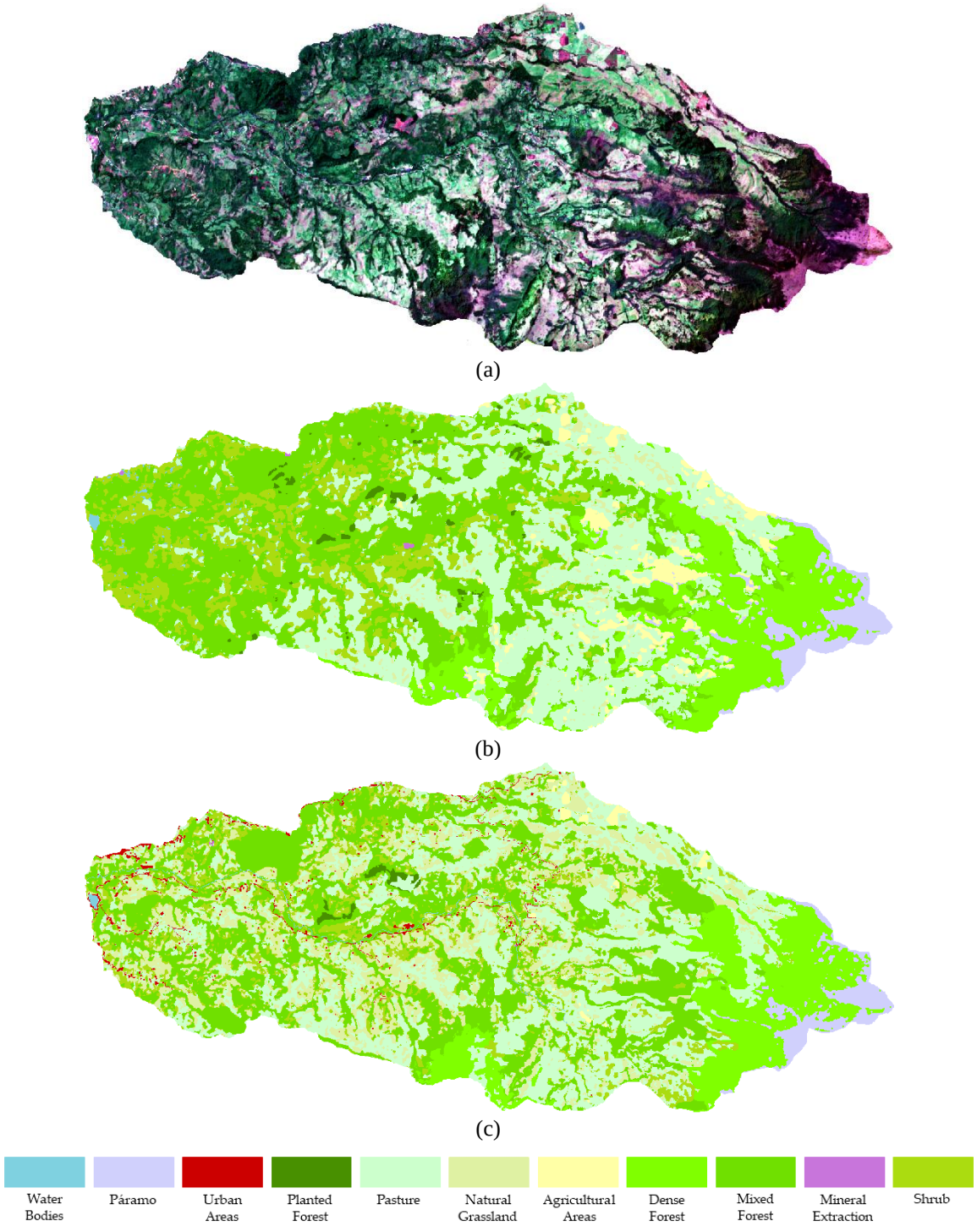

Figure 3. LULC result for Las Piedras River sub-basin: (a) Sentinel-2 natural color image; (b) LULC map with a 11x11 kernel; (c) LULC map with a 3x3 kernel.

REFERENCES

[1] Oswald, S. M., Hollosi, B., Žuvela-Aloise, M., See, L., Guggenberger, S., Hafner, W., Prokop, G., Storch, A. and Schieder, W., "Using urban climate modelling and improved land use classifications to support climate change adaptation in urban environments: A case study for the city of Klagenfurt, Austria," Urban Climate **31**(100582), 16 (2020).

[2] Benhammou, Y., Alcaraz-Segura, D., Guirado, E., Khaldi, R., Achchab, B., Herrera, F. and Tabik, S., "Sentinel2GlobalLULC: A Sentinel-2 RGB image tile dataset for global land use/cover mapping with deep learning," 1, Sci Data **9**(1), 20 (2022).

[3] Carranza-García, M., García-Gutiérrez, J. and Riquelme, J. C., "A Framework for Evaluating Land Use and Land Cover Classification Using Convolutional Neural Networks," 3, Remote Sensing **11**(3), 274 (2019).

[4] Chuvieco, E., Li, J. and Yang, X., eds., [Advances in Earth Observation of Global Change, 1st ed.], Springer Netherlands, Dordrecht (2010).

[5] Smyth, T. A. G., Wilson, R., Rooney, P. and Yates, K. L., "Extent, accuracy and repeatability of bare sand and vegetation cover in dunes mapped from aerial imagery is highly variable," Aeolian Research **56**, 100799 (2022).

[6] Lilay, M. Y. and Taye, G. D., "Semantic segmentation model for land cover classification from satellite images in Gambella National Park, Ethiopia," SN Appl. Sci. **5**(76), 15 (2023).

[7] Yuh, Y. G., Tracz, W., Matthews, H. D. and Turner, S. E., "Application of machine learning approaches for land cover monitoring in northern Cameroon," Ecological Informatics **74**, 101955 (2023).

[8] Keshtkar, H., Voigt, W. and Alizadeh, E., "Land-cover classification and analysis of change using machine-learning classifiers and multi-temporal remote sensing imagery," Arab J Geosci **10**(154), 154 (2017).

[9] Pencue-Fierro, E. L., Solano-Correa, Y. T., Corrales-Muñoz, J. C. and Figueroa-Casas, A., "A Semi-Supervised Hybrid Approach for Multitemporal Multi-Region Multisensor Landsat Data Classification," IEEE Journal of Selected Topics in Applied Earth Observations and Remote Sensing **9**(12), 5424–5435 (2016).

[10] Swetanisha, S., Panda, A. R. and Behera, D. K., "Land use/land cover classification using machine learning models," 2, International Journal of Electrical and Computer Engineering (IJECE) **12**(2), 2040–2046 (2022).

[11] Park, J., Lee, Y. and Lee, J., "Assessment of Machine Learning Algorithms for Land Cover Classification Using Remotely Sensed Data," Sensors and Materials **33**(11), 3885 (2021).

[12] Razafinimaro, A., Hajalalaina, A. R., Rakotonirainy, H. and Zafimarina, R., "Land cover classification based optical satellite images using machine learning algorithms," 3, International Journal of Advances in Intelligent Informatics **8**(3), 362–380 (2022).

[13] Simón Sánchez, A.-M., González-Piqueras, J., de la Ossa, L. and Calera, A., "Convolutional Neural Networks for Agricultural Land Use Classification from Sentinel-2 Image Time Series," 21, Remote Sensing **14**(21), 5373 (2022).

[14] Zhang, W., Tang, P., Corpetti, T. and Zhao, L., "WTS: A Weakly towards Strongly Supervised Learning Framework for Remote Sensing Land Cover Classification Using Segmentation Models," 3, Remote Sensing **13**(3), 394 (2021).

[15] Pedrayes, O. D., Lema, D. G., García, D. F., Usamentiaga, R. and Alonso, Á., "Evaluation of Semantic Segmentation Methods for Land Use with Spectral Imaging Using Sentinel-2 and PNOA Imagery," 12, Remote Sensing **13**(12), 2292 (2021).

[16] Kroupi, E., Kesa, M., Navarro-Sánchez, V. D., Saeed, S., Pelloquin, C., Alhaddad, B., Moreno, L., Soria-Frisch, A. and Ruffini, G., "Deep convolutional neural networks for land-cover classification with Sentinel-2 images," JARS **13**(2), 024525 (2019).

[17] J. Louis, O Devignot, and L. Pessiot., "Level-2A Algorithm Theoretical Basis Document," Technical report, 78 (2021).

[18] López, I. D., Figueroa, A. and Corrales, J. C., "Multi-Dimensional Data Preparation: A Process to Support Vulnerability Analysis and Climate Change Adaptation," IEEE Access **8**, 87228–87242 (2020).

[19] Ren, H. and Feng, G., "Are soil-adjusted vegetation indices better than soil-unadjusted vegetation indices for above-ground green biomass estimation in arid and semi-arid grasslands?," Grass and Forage Science **70**(4), 611–619 (2015).

[20] Baret, F. and Guyot, G., "Potentials and limits of vegetation indices for LAI and APAR assessment," Remote Sensing of Environment **35**(2), 161–173 (1991).

[21] Huete, A., Didan, K., Miura, T., Rodriguez, E. P., Gao, X. and Ferreira, L. G., "Overview of the radiometric and biophysical performance of the MODIS vegetation indices," Remote Sensing of Environment **83**(1), 195–213 (2002).

[22] Hunt Jr., E. R., Daughtry, C. S. T., Eitel, J. U. H. and Long, D. S., "Remote Sensing Leaf Chlorophyll Content Using a Visible Band Index," Agronomy Journal **103**(4), 1090–1099 (2011).

[23] Nouaim, W., Chakiri, S., Rambourg, D., Karaoui, I., Ettaqy, A., Chao, J., Allouza, M., Razoki, B., Yazidi, M. and El Hmidi, F., "Mapping the water erosion risk in the Lakhdar river basin (central High Atlas, Morocco)," Geology, Ecology, and Landscapes **3**(1), 22–28 (2019).
[24] Gao, B., "NDWI—A normalized difference water index for remote sensing of vegetation liquid water from space," Remote Sensing of Environment **58**(3), 257–266 (1996).
[25] Dogan, H. M., "Applications of remote sensing and Geographic Information Systems to assess ferrous minerals and iron oxide of Tokat province in Turkey," International Journal of Remote Sensing **29**(1), 221–233 (2008).
[26] Yan, C., Fan, X., Fan, J., Yu, L., Wang, N., Chen, L. and Li, X., "HyFormer: Hybrid Transformer and CNN for Pixel-Level Multispectral Image Land Cover Classification," 4, International Journal of Environmental Research and Public Health **20**(4), 3059 (2023).
[27] Lecun, Y., Bottou, L., Bengio, Y. and Haffner, P., "Gradient-based learning applied to document recognition," Proceedings of the IEEE **86**(11), 2278–2324 (1998).
[28] Yang, C., Rottensteiner, F. and Heipke, C., "CLASSIFICATION of LAND COVER and LAND USE BASED on CONVOLUTIONAL NEURAL NETWORKS," presented at ISPRS Annals of the Photogrammetry, Remote Sensing and Spatial Information Sciences, 2018, 251–258.
[29] "The Sequential model | TensorFlow Core.", TensorFlow, <bit.ly/3Fr9qPP> (15 March 2023).
[30] Ruiz O., D. M., Idrobo M., J. P., Otero S., J. D. and Figueroa C., A., "Effects of Productive Activities on the Water Quality for Human Consumption in an Andean Basin, a Case Study," Revista Internacional de Contaminación Ambiental **33**(3), 361–375 (2017).
[31] Phiri, D., Simwanda, M., Salekin, S., Nyirenda, V. R., Murayama, Y. and Ranagalage, M., "Sentinel-2 Data for Land Cover/Use Mapping: A Review," 14, Remote Sensing **12**(14), 2291 (2020).
[32] Essien, P., Figueiredo, C. A. O. B., Takahashi, H., Klutse, N. A. B., Wrasse, C. M., Afonso, J. M. de S., Quispe, D. P., Lomotey, S. O., Ayorinde, T. T., Sobral, J. H. A., Eghan, M. J., Sackey, S. S., Barros, D., Bilibio, A. V., Nkrumah, F. and Quagraine, K. A., "Intertropical Convergence Zone as the Possible Source Mechanism for Southward Propagating Medium-Scale Traveling Ionospheric Disturbances over South American Low-Latitude and Equatorial Region," 11, Atmosphere **13**(11), 15 (2022).
[33] European Space Agency (ESA)., "Copernicus Open Access Hub," <https://scihub.copernicus.eu/dhus/#/home> (29 March 2023).
[34] Alaska Satellite Facility., "ASF Data Search," <https://search.asf.alaska.edu/#/> (29 March 2023).
[35] Muñoz-Ordóñez, J., Cobos, C., Mendoza, M., Herrera-Viedma, E., Herrera, F. and Tabik, S., "Framework for the Training of Deep Neural Networks in TensorFlow Using Metaheuristics," Intelligent Data Engineering and Automated Learning – IDEAL 2018, H. Yin, D. Camacho, P. Novais, and A. J. Tallón-Ballesteros, Eds., 801–811, Springer International Publishing, Cham (2018).
[36] Zanaga, D., Van De Kerchove, R., Daems, D., De Keersmaecker, W., Brockmann, C., Kirches, G., Wevers, J., Cartus, O., Santoro, M., Fritz, S., Lesiv, M., Herold, M., Tsendbazar, N.-E., Xu, P., Ramoino, F. and Arino, O., "ESA WorldCover 10 m 2021 v200" (2022).